M. Civati, L. Sartori, A. Croce
Design of a Two-Bladed 10 MW Rotor with Teetering Hub
Journal of Physics: Conference Series, Vol. 1037, 2018, 042007 (10 pages)
doi:10.1088/1742-6596/1037/4/042007

Design of a two-bladed 10 MW rotor with teetering hub

IOP Conf. Series: Journal of Physics: Conf. Series **1037** (2018) 042007 doi:10.1088/1742-6596/1037/4/042007

Design of a two-bladed 10 MW rotor with teetering hub

M Civati, L Sartori and A Croce

Dipartimento di Scienze e Tecnologie Aerospaziali, Politecnico di Milano, Via La Masa 34, 20156 Milano, Italy

E-mail: alessandro.croce@polimi.it

Abstract. Two-bladed rotors are emerging as a viable alternative to classic three-bladed ones for driving down the cost of energy of large sized wind turbines. By eliminating a blade one could easily reduce the cost of the rotor. However, design challenges arise due to the reduced power output and the resonance typically occurring between the frequency of the tower and the two-per-revolution. In this work, we perform a dedicated design of a two-bladed configuration for a 10 MW wind turbine: the solution is upwind and equipped with a teeter hinge at the hub in order to alleviate the loads on the fixed infrastructure. The rotor and the tower are then optimized by using a holistic design algorithm, and a complete technical and economic assessment of the optimal design is conducted against a reference three-bladed one in order to compare the main performance including loads, energy yielding and the cost of energy.

1. Introduction

The design of next-generation wind turbines requires to drive down the cost of energy as much as possible in order to make wind energy competitive against traditional energy sources. As the size and complexity of the rotors increase, the research deals with alternative concepts to the classic upwind, three-bladed rotor as a way to cut the capital cost of wind plants. In this view, two-bladed rotors have been proposed as a possible way to design very large turbines, since by leaving out one of the blades it is theoretically possible to reduce the cost of the rotor by one-third. Two-bladed rotors, however, require a higher rotational speed to optimally produce power, since the lower rotor solidity requires the TSR to be higher than typical three-blades values [1]. This also prevents a full exploitation of these turbines in onshore, where the acoustic emissions due to the rotational speed are an issue in the majority of applications.

In the literature there is a renewed interest in two-bladed wind turbines and detailed loading comparisons have been conducted between two and three-bladed rotors [2], whereas dedicated control strategies have been recently proposed as a way to mitigate loads [3, 4]. Moreover, in the last few years, several industrial projects have been presented showing the interests towards this two-bladed configuration.

However, the design implications of a two-bladed rotor against a three-bladed still need to be investigated in depth. In particular, the energy drop due to the lower solidity as well as the resonance typically occurring between the natural frequencies of the tower and the 2P [5] need to be investigated properly in the context of a multi-disciplinary design procedure. In this paper, we perform the design of an upwind two-bladed wind turbine with a teetering hub. The design is obtained through an aero-structural optimization of blade and tower and it is subsequently

IOP Conf. Series: Journal of Physics: Conf. Series **1037** (2018) 042007 doi:10.1088/1742-6596/1037/4/042007

compared against a reference three-bladed in order to identify strengths and weaknesses of the concept, and to assess the economic viability of the solution.

2. Methodology

In this paper, the design is carried out by the holistic optimization tool `Cp-Max` [6]. The initial Baseline is a two-bladed version of the INNWIND.EU 10 MW wind turbine: at this stage, one of the blades is simply removed and the characteristics of the remaining blades are not redesigned, whereas a teeter hinge is defined at the hub to alleviate the unbalanced loading at the rotor disk. The mechanical behavior of this teeter hinge, which includes a spring and a damper, has been defined by the authors based on their experience maturated within previous industrial projects, in order to have feasible characteristics. For the same reason, in this work the design has been conducted on an upwind configuration, leaving the analysis on a downwind rotor for future works.

The wind turbine is represented through a multi-body modelling of the system, so that the teeter hinge can be simply defined by a revolute joint with its associated properties of stiffness and damping. Two teeter ends are defined to limit the possible excursions of the hinge and to prevent fatal impacts between the blades and the tower. Starting from the Baseline, the target value of the rotor solidity was gradually increased. For each solution, an aerodynamic redesign was performed by the dedicated submodule of `Cp-Max`, so that the chord and twist could be redesigned to give the maximum AEP for a certain solidity. Afterwards, the process continued with the optimization of prebend and spar caps, resulting in further reductions of the cost of energy. The final study is about the tower: first a verified model for the reference three-bladed turbine is obtained, and then different innovative constructive solutions act to solve problems deriving from fatigue loads are studied for the two-bladed turbine. Finally, a cost of energy analysis has been performed, in order to quantify the improvements with respect to the baseline.

3. Model Description

The starting point of this work is based on the three-bladed 10MW INNWIND.EU wind turbine, whose principal characteristics are showed in Table 1. In particular the three-bladed model, from now referred as 3B Reference, is obtained only with small adjustments of the structural elements distribution, while the henceforth called 2B Baseline considers also a teetering hub.

Table 1: INNWIND.EU wind turbine principal characteristics.

Rated power [MW]	10
Rotor diameter [m]	178.3
Hub diameter [m]	5.6
Hub height [m]	119
Shaft tilt angle [deg]	5
Rotor precone angle [deg]	2.5

3.1. Teeter Hinge

A two-bladed wind turbine with rigid hub presents some disadvantages, caused mainly by the rotational asymmetry of the rotor. This characteristic, in addition with the action of the wind shear, generates extra bending moment on the hub with the same frequency of the rotation (2P);

together with the loads deriving from yaw maneuvers with horizontal blades, the result is a huge increment in the fatigue loads of the turbine, specially for blade root, hub and tower. It can be seen that there are larger number and magnitudes of the harmonic components comparing to the three-bladed turbine, and this leads to resonant couplings in the mode shapes. These couplings arise when the rotor speed is such that frequencies of different modes get closer [5].

The presence of a teeter hinge between the rotor and the hub can mitigate these uneven loads. This allows the rotor to rotate in the fore-aft direction, reducing the out-of-plane bending moment fluctuations. In practice, this hinge is linked to a rotational spring, with the task of responding to the fluctuations and controlling the excursion. Furthermore, in order to avoid risk of clashes between blades and tower, the motion is limited by a teeter end impact, so a maximal teeter angle must not be exceeded. This is a safety measure, but is inadvisable to leave the turbine works at this point, unless in case of start up or shut down, because a teeter end impact causes additional bending moments and so increase the fatigue loads.

In the literature, different studies about the ranges of work of teeter hinges can be found. In particular, they are divided based on the restraint torque, and they include a free-zone followed by different types of end impacts, divided in soft, hard and ultra stop [7] [8]. In this work, the operating range is chosen without a free teeter one. As shown in Figure 1, there is a restraint torque of 1.8e06 Nm/deg from $0°$ to $11°$, referred as soft teeter range, then a hard stop is implemented up to $13°$ with a torque of about 9.6e07 Nm/deg. Even if the verification of this important mechanical system is out of the scope of this paper, these values are important in order to have realistic aeroelastic loads on the systems and hence to have realistic rotor and tower design. For this reason, these characteristics have been obtained throughout a scale up procedure, which started from real mechanical characteristics based on some previous industrial projects where the authors have been involved.

With this choice of ranges and torques, all the simulations performed in the following will maintain the teeter angle in the soft range, without ever reaching the hard stop. This permits to avoid extra loads due to the teeter end impact, although we are fully aware that a larger set of DLCs could lead to occasional teeter-end impacts. This consideration will be the basis of a dedicated study in the future. For completeness, two characteristic angles are extrapolated from the simulations and they shown in Table 2. The first value is the teeter angle corresponding to the case of maximum tip deflection, while the second value is the overall maximum teeter angle from all the simulations.

Looking at the modes of the wind turbine, the addition of the teeter hinge, which implement a further degree of freedom, generates a new mode. The frequency of this mode is just below the rotational frequency (1P) but it is lagging of about 90 degree [9].

Table 2: Characteristic teeter angles.

Condition	DLC	Description	Teeter Angle [°]
Maximum tip deflection	DLC 1.3	ETM at 11 m/s	3.4°
Worst case	DLC 2.3	EOG at rated speed with grid loss	7.9°

3.2. Models Comparison

The power that can be extracted from the turbine depends on the overall rotor solidity. Indeed, in the 2B Baseline there is a huge reduction of the optimal power coefficient (C_p^*), which is compared against the 3B Reference in Figure 2. Additionally, the shift of the envelope of the

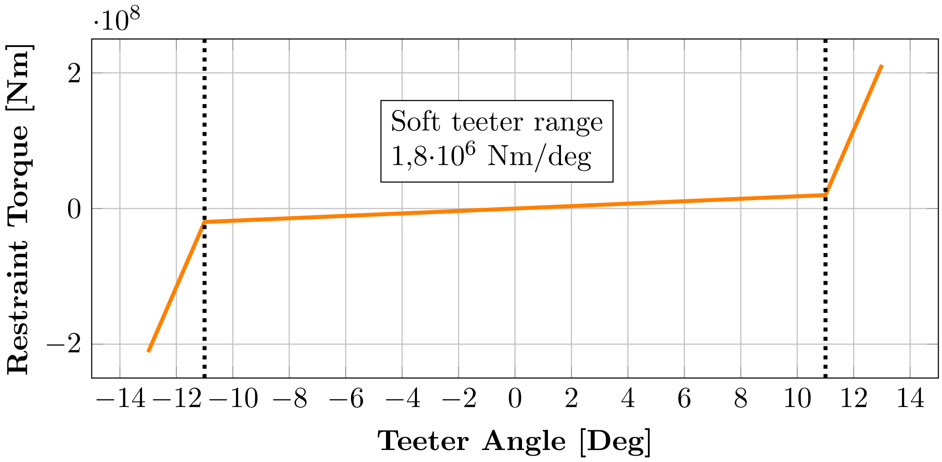

Figure 1: Teeter restraint characteristics.

Cp-TSR curves towards higher tip-speed ratios brings the wind turbine to work at a higher rotational speed, which can also imply reaching the tip speed constraint in onshore wind plants. This is clearly evident in the limited Cp between 9-11 m/s for the 2B Baseline. This global drop in power contributes to the reduction of the annual energy production (AEP) of about 3.5 % (Figure 3). All these parameters are shown in Table 3.

The main differences which characterize the blades of the two models are due to the new total blade deflection generated by the addition of the teeter hinge. This has led to a thickening of the 2B Baseline spar caps, and consequently to an increment in total blade mass compared to the 3B Reference model of about 14 %. The comparison between the ultimate loads experienced by the wind turbine components is shown in Figure 4. The most important information extractable from these plots is the huge reduction of the ultimate loads at the hub and tower top: this is due to the intervention of the teeter hinge, which absorbs most of the loads transmitted by the blades. A comparison of the fatigue loads is shown in Figure 5: in particular it can be noted a dramatic increment of the tower root FA and SS DELs. This is due to the different blade-passing frequency of the two-bladed wind turbine, which couples to the tower frequency and produces resonance phenomena.

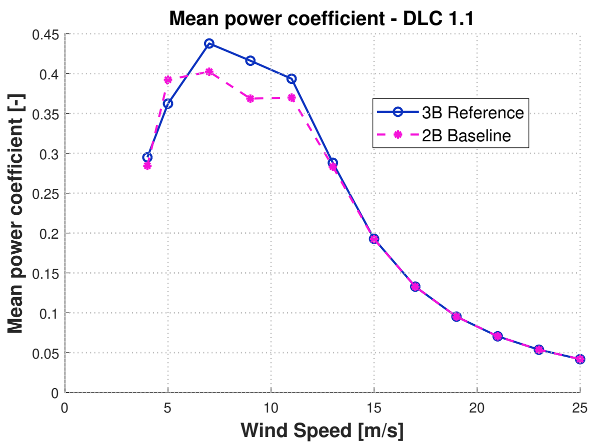

Figure 2: Power coefficient comparison.

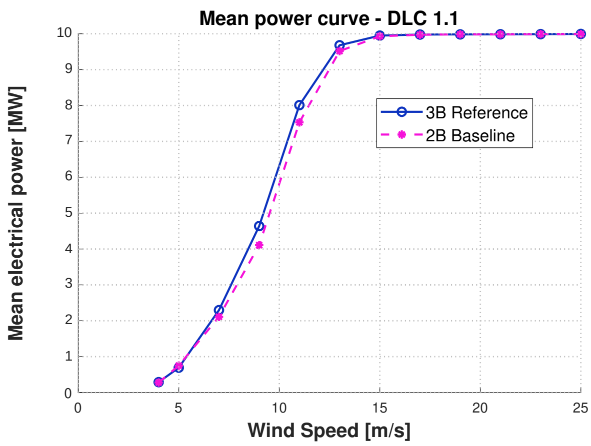

Figure 3: Turbulent power curve comparison.

Table 3: Regulation parameters comparison.

	C_p^* [-]	Ω_{rated} [rpm]	V_{rated} [m/s]	TSR^* [-]	AEP [GWh/yr]
3B Reference	0.4581	9.17	11.49	7.45	46.26
2B Baseline	0.3907	9.64	9.95	9.05	44.64

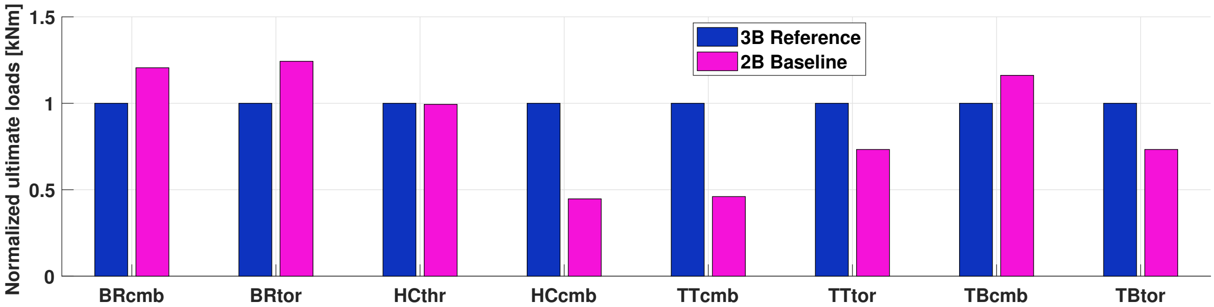

Figure 4: Comparison of ultimate loads between the 3B Reference and the 2B Baseline. BR is blade root, HC is hub center, TT is tower top and TB is tower base. **cmb** is the multi-directional bending, **thr** is thrust and **tor** is torsion.

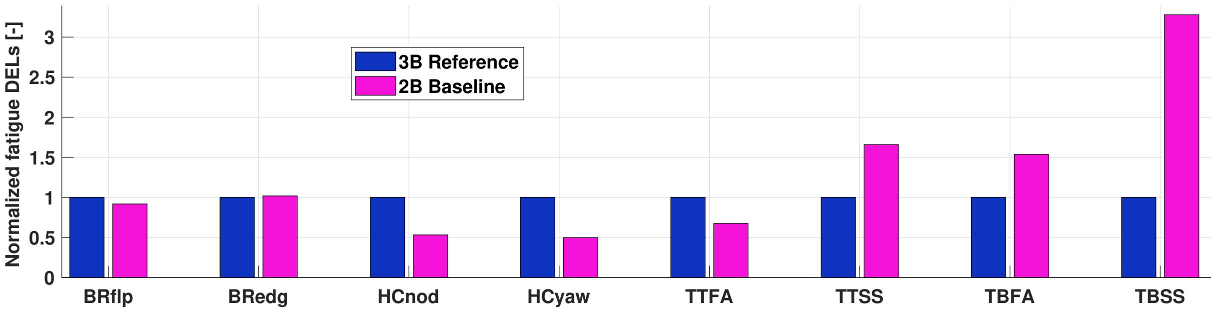

Figure 5: Comparison of fatigue loads between the 3B Reference and the 2B Baseline. BR is blade root, HC is hub center, TT is tower top and TB is tower base. **flp** is flapwise, **edg** is edgewise, **nod** is nodding, **yaw** is yawing and **FA**, **SS** are fore-aft and side-side.

4. Rotor Optimization

Starting from these considerations, we now focus on the redesign of the rotor. The process can be summarized in three different activities: increase the blade planar solidity, optimization of the prebend and blade structural optimization with independent spar caps thicknesses, with the last two steps performed at the same time. The idea of this optimization process is to work on single design solutions for every step, choosing at each time the best fitting configuration and go on that way. With this step by step approach, there is the possibility to follow a good optimization path, avoiding unnecessary studies and solutions, and reaching optimal configurations in limited computational time. For the scope of this work, this approach is preferred instead of a classical optimization process which takes into account all the design variables at the same time.

4.1. Planar Solidity Augmentation

The rotor planar solidity is a very important parameter for the wind turbine, because it directly affects the aerodynamic performances and the operating conditions. Therefore the idea is to increase this value in order to reduce the overall cost of energy of the machine.

As it can be seen in Figure 6, the increase in chord is concentrated in the region near 30 % of the span, where the airfoils are thicker. From this new geometry, the Cp-TSR curves tend to move toward lower values of tip speed ratio (TSR) and the blade stiffness increases due to the wider and thicker structure; consequently there is an increase of the rated speed (V_r). The secondary effect is proved by the huge reduction of mass, due to the lighter need for structural stiffening. As expected, also the AEP grows and consequently the cost of energy follows a downward curve. These results are shown in Figure 7, reported as percentage variation from the initial 2B Baseline model. The solution with a 16% higher solidity led to the best COE reduction (approximately 1%) and therefore it will be used in the next steps.

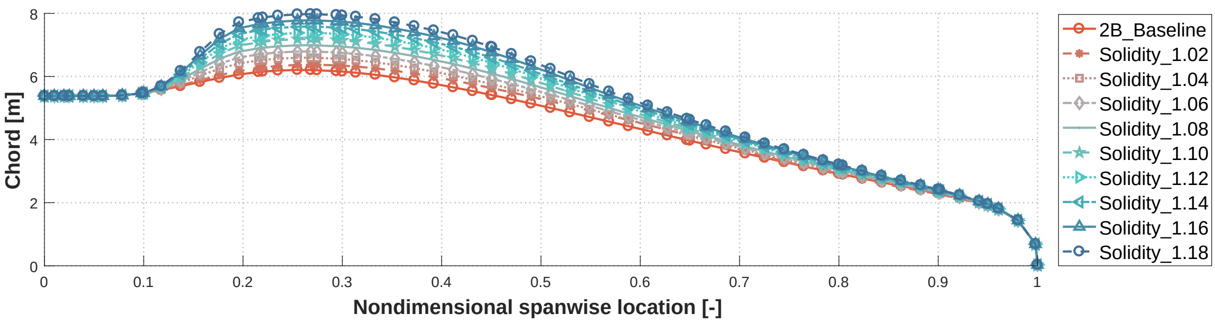

Figure 6: Optimal chord for increasing values of rotor solidity.

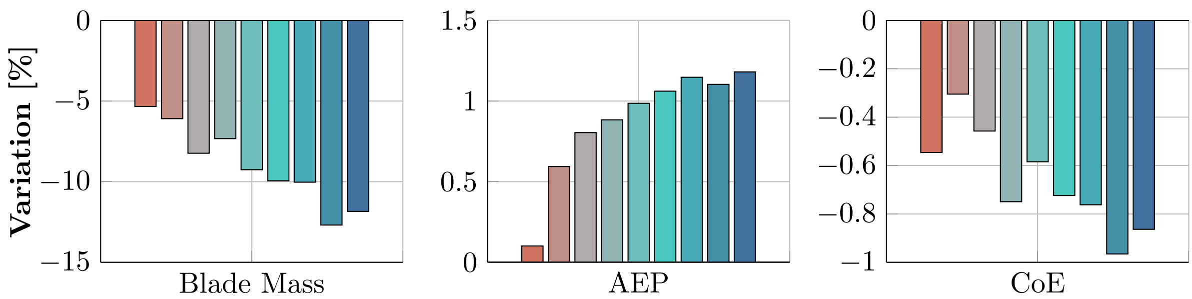

Figure 7: Blade mass, AEP and CoE variations with respect to the 2B Baseline.

4.2. Prebend and Spar Caps Optimization

The prebend optimization is implemented through the dedicated submodule [10], and at the same time the structural loop is executed treating PS and SS spar caps as independent design variables. The optimization of the blade prebend is performed with the aim of extract the maximum energy from the wind. The original value of the prebend was fitted during the solidity augmentation, while in the preliminary design of the 2B Baseline an increment in stiffness was encountered. This led to a new prebend distribution, lower than the original, with a tip value of 4.361 m, as depicted in Figure 8.

For the spar caps optimization, since the major loads and deflections occur in the wind direction, the SS thickness distribution presents a huge reduction concentrated in the second half of the blade span, visible in Figure 9.

The final variations for blade mass, AEP and cost of energy in respect to the 2B Baseline values are summarized in Table 4. The final cost of energy is represented by a reduction from the 2B Baseline of about 1.30 %.

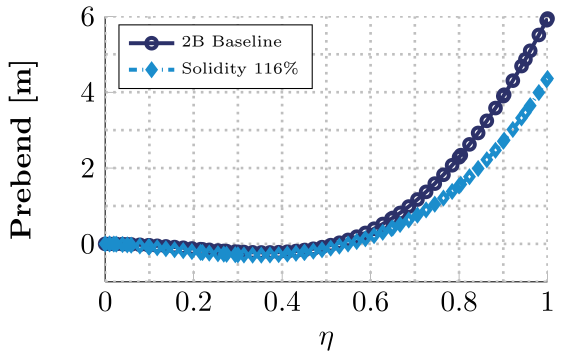

Figure 8: Prebend distribution comparison.

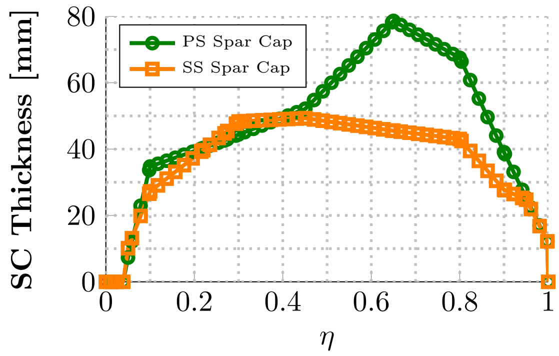

Figure 9: Spar Caps thickness distribution.

Table 4: Blade mass, AEP and CoE values and variations for the prebend and spar caps optimization.

	Mass [kg]	Δ [%]	AEP [GWh/yr]	Δ [%]	CoE [$/MWh]	Δ [%]
2B Baseline	45183	-	44.64	-	78.73	-
Solidity 116%	38090	-15.70	45.46	1.84	77.71	-1.30

5. Tower Optimization

A very important consideration in the design of wind turbine is the coupling between the tower natural frequencies and the rotor fluctuations at rotational or blade-passing frequency. In order to avoid resonance phenomena derived from these couplings, the tower frequencies must stay at some distance from the characteristic frequencies, mainly in the region near the rated rotor speed. For this reason, three types of towers can be designed: stiff towers with natural frequency greater than the blade-passing frequency, soft-soft towers with natural frequency lower than rotational frequency, and soft towers with natural frequency between the previous two. Most of the towers, including the one of this paper, are designed to work in the range between the characteristic frequencies, and therefore are considered as soft towers.

5.1. Three-Bladed Wind Turbine Tower

For the three-bladed wind turbine, the characteristic frequencies could be identified in the 1P and the 3P. In this case the possible working range for the tower is quite large, as it can be seen in Figure 10, and allows to avoid pretty easily the resonance phenomena. After a thorough structural verification and optimization, the resulting tower for the 3B Baseline has become about 39 % heavier.

5.2. Two-Bladed Wind Turbine Tower

When dealing with a two-bladed configuration, the characteristic frequencies to be monitored are the 1P and the 2P. The increase in the tower DELs is due to the higher energy content in the turbulent wind field, which makes the 2P the dominant frequency that interacts with the tower mode frequency. Therefore, the soft working range available for the three-bladed rotor is now very limited, and the possibility to design a soft tower becomes very challenging. Indeed, in the minimal available bandwidth between the frequencies, it is problematic to verify the tower, because of the reduced dimension of thickness and diameter. At this point, the only feasible way to obtain a verified two-bladed wind turbine tower is to raise the frequencies up above the 2P (Figure 11), in the stiff working range. As we completed the structural optimization loop on the last and best rotor configuration, the sizing was determined by the fatigue loads, due to the resonance phenomena, and the final tower has become about 87 % heavier.

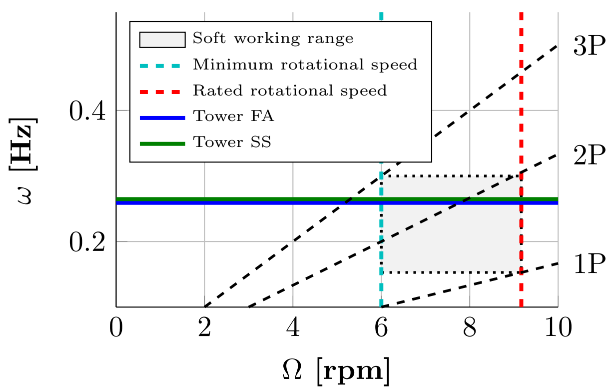

Figure 10: 3B tower modes and working range.

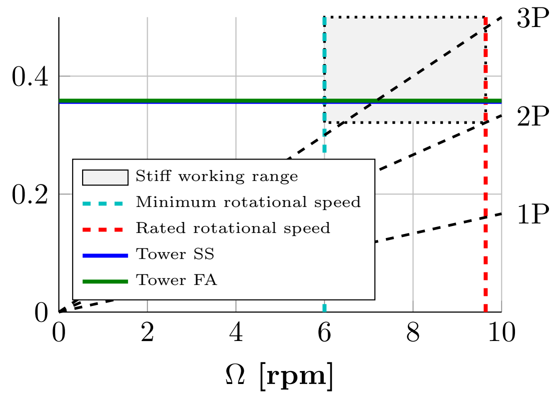

Figure 11: 2B tower modes and working range.

5.3. Tuned Mass Damper

A method to reduce vibrations is to introduce a tuned mass damper (TMD) positioned at the top of the tower. The TMD has to be tuned by choosing mass and spring such that its natural frequency is the same as that of the system. The effect of this application is that the natural frequency of the system is replaced by two new other frequencies, located at the sides of the previous one.

Referring to studies about structural control of wind turbines [11], the mass of the TMD should be approximately 2 % of the tower and therefore in this work the chosen value is 20 ton. Considering that the mass could be a container filled with water, the TMD can be synthesized in a sphere with about 1.7 m of radius. In the model it is implemented for both the principal directions, fore-aft and side-side. The resulting constant is of 8e04 N/m and the effect of the TMD is well visible in Figure 12, where now the tower modes have doubled and lie under and over the 2P at rated rotational speed. The damper is chosen in order to limit the maximum excursion of the TMD, and a safety measure to avoid the collision with the inner tower edges is actuated by enlarging the top diameter and adding a hard stop impact like in the teeter hinge case, with a restraint force of 1.35e06 N/m. Downstream of the simulations, the TMD remains always in the soft range.

The main results are presented in Table 5: the comparison between the tower root loads shows that the side-side DEL has been reduced of 42.19 % while the fore-aft DEL of only 16.7 %. This difference is probably due to the fact that the SS component of the loads has only alternate component, while the FA case include also a mean value of the stress, which does not depend from vibrations.

At a design level, it can be seen that after the introduction of the TMD it was possible to reduce the tower mass of 22 % and the cost of energy of about 1 %. However, the cost of the TMD is not taken into account.

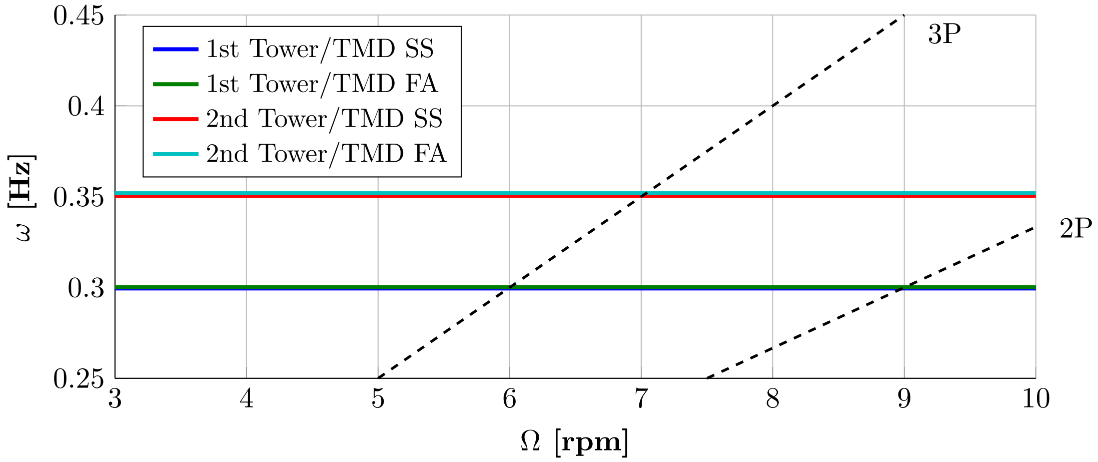

Figure 12: Two-bladed tower and TMD coupled modes.

Table 5: Tower root DELs summary comparison between two-bladed tower with and without the TMD.

DEL	w/o TMD	w/ TMD	Δ [%]
Fore-Aft [kNm]	323925.12	269823.19	-16.70
Side-Side [kNm]	335601.15	194007.20	-42.19

5.4. External Post-Tensioning Tendons

In a wide range of civil structures, such as buildings, bridges and dams, pre-stressed concrete is used in order to improve the performances. This is obtained by tensioning strands cables before (pre-tension) or after (post-tension) the cast of the concrete; here the tower is made of steel, so the idea is to use a lighter tower and compensate the lack of stiffness introducing these high tensile steel cables, in order to maintain the tower frequencies above the 2P.

The aim of the post-tensioning is not to compress the structure, but simply to avoid the possible tensile loss due to tower deformations: a too marked post-tensioning could reduce the tower frequencies. After an analysis of the tower top movements, the value chosen for the cables stressing is only 10 cm, and does not affect the tower frequencies significantly.

In practice these cables could be positioned along the inner tower wall, on the whole circumference, and extended from the tower root to the top. In the multi-body model they are simplified into four springs.

Three different cabled towers are studied, in which the diameter distribution is varied and the structural optimization submodule optimizes the thicknesses to satisfy the constraints. It is remarkable to notice that in this case, buckling has become the predominant constraint in the upper area of the tower instead of fatigue. The idea is to size the spring constant in order to reach a frequency above the 2P; this is obtained by a trial-and-error procedure, in which the value of the spring constant has been parametrically changed until the desired frequency was obtained. These solutions are summarized in Table 6, and all of them are well below the 3B Reference tower mass of 873259 kg.

This is only a preliminary study and it does not take into account the mass and the costs of the cables.

Table 6: Tower different masses, initial frequencies and spring constants.

	Mass [kg]	Frequency [Hz]	Spring constant [kN/m]
Tower 1	841151	0.265	2.8e06
Tower 2	797354	0.289	1.8e06
Tower 3	821360	0.306	1.2e06

6. Conclusions

In this work, we have designed a two-bladed 10 MW wind turbine with teetering hub. A preliminary aero-structural rotor optimization performed with dedicated design algorithms allowed to obtain a two-bladed solution which seems attractive when compared against a three-bladed turbine of the same size. However, high fatigue loads due to resonance led the tower design to be very stiff, resulting in a high tower mass and a global worsening of the cost of energy. This also highlights the need of dedicated solutions for the design of the tower.

Summarizing the results, it has been found that the applied procedures are directly linked to mass reduction, increase in annual energy production, and so lowering of the cost of energy. However, the evaluation of the cost of energy gives just an overview on the likely production, transportation, construction and maintenance costs of the wind turbine. Indeed, the considered cost model is mostly suitable only for basic three-bladed wind turbines. In the case in question, the cost model should include several corrections, some in favour and others against the two-bladed wind turbine. The costs of the teeter hinge, along with the tuned mass damper and the external post-tensioning tendons are not taken into account. In addition, it is possible to have more cost savings, considering that a two-bladed rotor can be mounted directly on the ground or, in case of offshore applications, it can be preassembled with the nacelle and transported more easily.

References

[1] Jamieson P 2011 *Innovation in wind turbine design* John Wiley & Sons Ltd
[2] Bergami L, Madsen H Aa and Rasmussen F 2014 A Two-Bladed Teetering Hub configuration for the DTU 10 MW RWT: loads considerations *Proc. of EWEA 2014*
[3] van Solingen E, Beerens J, Mulders S P, De Breuker R and van Wingerden J W 2016 Control design for a two-bladed downwind teeterless damped free-yaw wind turbine *Mechatronics* **36** 77-99
[4] Riboldi C E D and Cacciola S 2017 Individual pitch control for 2-bladed wind turbines via multiblade multilag transformation *Wind Energy* **20** 1955-1969
[5] Hansen M H 2016 Modal dynamics of structures with bladed isotropic rotors and its complexity for two-bladed rotors *Wind Energy Science* **1** 271–296
[6] Bortolotti P, Bottasso C L and Croce A 2016 Combined preliminary-detailed design of wind turbines *Wind Energy Science* **1** 71-88
[7] Schorbach V, Dalhoff P and Gust P 2014 Taming the inevitable: significant parameters of teeter end impacts *J. Phys.: Conf. Series* **524**(1) 012070
[8] Schorbach V, Haines R and Dalhoff P 2015 Teeter end impacts: analysis and classification of most unfavourable events *Wind Energy* **19** 115–131
[9] Bir G S and Stol K 1999 Operating Modes of a Teetered-Rotor Wind Turbine *Int. Modal Analysis Conf.*
[10] Sartori L, Bortolotti P, Croce A and Bottasso C L 2016 Integration of prebend optimization in a holistic wind turbine design tool *TORQUE*
[11] Lackner M A and Rotea M A 2010 Passive structural control of offshore wind turbines *Wind Energy* **14** 373–388